Available online at www.sciencedirect.com
SCIENCE DIRECT
ELSEVIER
Polymer 46 (2005) 2872–2879
polymer
www.elsevier.com/locate/polymer

Hybrid nanocomposites containing silica and PEO segments: preparation through dual-curing process and characterization

Giulio Malucelli[a,*], Aldo Priola[a], Marco Sangermano[a], Ezio Amerio[a], Elisa Zini[b], Elena Fabbri[c]

[a]*Dipartimento di Scienza dei Materiali e Ingegneria Chimica e Unità locale INSTM, Politecnico di Torino, C.so Duca degli Abruzzi 24, 10129 Torino, Italia*
[b]*Dipartimento di Dipartimento di Chimica 'G. Ciamician' e Unità Locale INSTM, Università di Bologna, Via Selmi 2, 40126 Bologna, Italia*
[c]*Dipartimento di Ingegneria dei Materiali e dell'Ambiente e Unità Locale INSTM, Università di Modena e Reggio Emilia, Via Vignolese 183, 41100 Modena, Italia*

Received 8 October 2004; received in revised form 4 February 2005
Available online 5 March 2005

Abstract

Hybrid organic–inorganic nanocomposites containing PEO segments linked to an acrylate–methacrylate network were prepared through a dual-curing process, involving photopolymerization and condensation of alkoxysilane groups. A Polyethyleneglycol 600 α,ω diacrylate (PEGDA 600) and a similar oligomer containing a Bisphenol A unit and α,ω methacrylate groups (BEMA 1400) were used. Mixtures of the oligomers together with methacryloyloxypropyltrimethoxysilane (MEMO) and tetraethoxysilane (TEOS) were prepared.

The kinetics of the reactions of photopolymerization and condensation was investigated. The conditions suitable for obtaining a complete conversion of both the reactive groups were settled up.

The obtained films were perfectly transparent and amorphous. The T_g values of the hybrids were found to increase by increasing the TEOS content and the alkoxysilane groups condensation.

TEM analyses indicated the formation of silica phases at a nanometric level; TGA curves revealed a higher thermal stability of the hybrid structures.

Keywords: Hybrid nanocomposites; UV curing; Alkoxysilanes condensation

1. Introduction

In the last few years new materials having a nanophasic morphology where an organic phase is strictly interconnected with an inorganic one (the so-called hybrid materials or ceramers) have been proposed and investigated [1,2]. These materials provide to combine the attractive properties of ceramics, such as thermal stability, high modulus and low coefficient of thermal expansion, with the high ductility and low temperature processing conditions of polymers.

The morphology of the nanophases strongly affects the properties and the behavior of the composites. These materials are very interesting in different fields such as for optical, mechanical, electronic and biomedical applications [3]. Their main commercial applications, at present, are in the field of protective coatings of both organic and inorganic substrates.

Several hybrids based on silica, TiO_2, ZnO, $CaCO_3$ have been investigated in the presence of different polymeric matrices [4–8]. The preferred way for their synthesis is the sol–gel process. It involves a two step hydrolysis and condensation reaction starting from metal alkoxides, as schematized in Fig. 1. Thus, organic–inorganic networks strictly interconnected are formed; they may result in dispersed nanostructured phases.

In particular silica/poly-ε-caprolactone hybrids were prepared and deeply investigated by Jerome and co-workers [9–12]. Similar systems were investigated by Pilati and co-workers, evidencing their flame retardancy and barrier properties [13].

Recently, hybrid organic–inorganic materials, obtained through a UV curing process, have been investigated. They combine the advantages connected to this technique, such as a rapid and solvent-free polymerization, with the sol–gel

* Corresponding author. Tel.: +39 011 564 4621; fax: +39 011 564 4699.
E-mail address: giulio.malucelli@polito.it (G. Malucelli).

0032-3861/$ - see front matter © 2005 Elsevier Ltd. All rights reserved.
doi:10.1016/j.polymer.2005.02.045

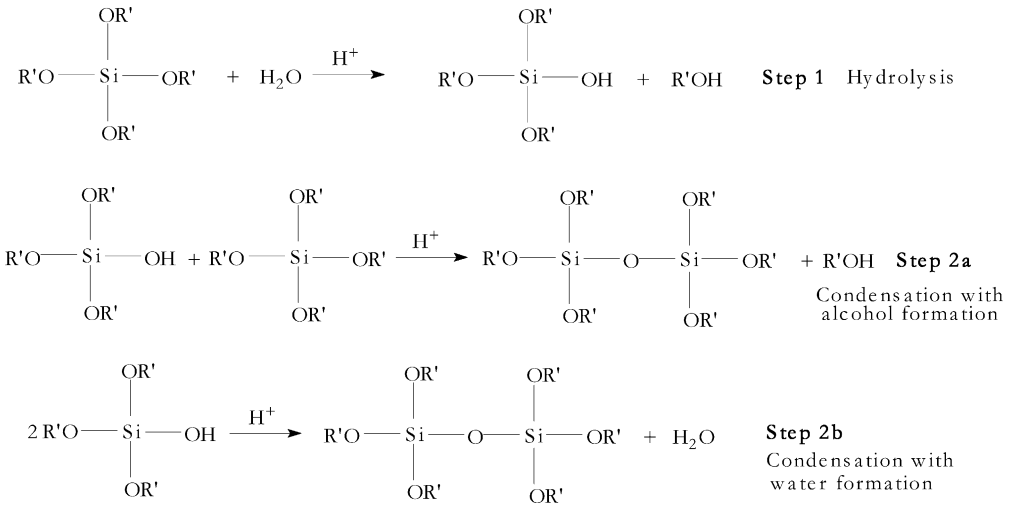

Fig. 1. Hydrolysis and condensation reactions involved in the sol–gel process.

advantages. Thus, it is possible to obtain coatings having improvements in different properties, such as resistance to scratching, abrasion, heat and radiation and other mechanical, electrical and optical properties [14–16].

In this context, we considered the preparation of new hybrid systems obtained by combining the UV curing process with the sol–gel reaction.

In the literature only a few papers on the preparation of nanocomposites through this dual-stage technique are reported. They investigate the preparation of hybrid organic–inorganic nanocomposites based on vinyltriethoxysilane, tetraethoxysilane and polyfunctional acrylates [17,18].

We have considered as organic precursors a Polyethyleneglycol 600 α,ω diacrylate (PEGDA 600) and an oligomer which can be considered as a modified PEGDA by inserting a Bisphenol A structure in the middle of the chain. The oligomer was ended by α,ω methacrylic groups (BEMA 1400).

These oligomers were added of methacryloyl-oxypropyl-trimethoxysilane (MEMO) as an organic–inorganic bridging monomer and of tetraethoxysilane (TEOS) as inorganic precursor.

The mixtures were subjected to the dual curing process, investigating the reaction conditions and the properties of the obtained cured products.

PEO acrylate oligomers were previously subjected to UV-curing and their properties evaluated [19].

2. Experimental

2.1. Materials

Polyethylenglycoldiacrylate (PEGDA 600) was kindly supplied by U.C.B. (Belgium). Bisphenol A ethoxylate (15 EO/phenol) dimethacrylate (BEMA 1400), methacryloyl-oxypropyl-trimethoxysilane (MEMO), tetraethoxysilane (TEOS), hydrochloric acid and dibuthyltin diacetate (condensation catalyst) were purchased from Aldrich. The structures of PEGDA 600 and BEMA 1400 are reported in Fig. 2; *n* is approximately 15 for both the monomers.

The following names were used in order to indicate the different mixtures:

- PEGDA 600, BEMA 1400: pure acrylate or methacrylate oligomers
- PEGDA, BEMA: mixtures of the acrylate or methacrylate oligomers with 20% w/w MEMO

As photoinitiator, 2-hydroxy-2-methyl-1-phenyl propan-1-one (Darocur 1173 from Ciba Specialty Chemicals) was employed.

2.2. Preparation of the hybrids

A typical UV-curable mixture was prepared by adding to PEGDA 600 or BEMA 1400 monomers, MEMO (14% w/w) and TEOS (30% w/w). The obtained mixture was added of 4% of Darocur 1173 as photoinitiator, 7% of water (alkoxy/water molar ratio = 2) and 2% of both dibutyltin diacetate and HCl conc., as condensation catalysts. Then it was coated on a PET substrate.

The photochemical curing was performed by using a medium vapor pressure Hg UV lamp (Helios Italquartz, Italy), with radiation intensity on the surface of the sample of 20 mW/cm^2, working in N_2 atmosphere [19].

The subsequent condensation reaction was performed treating the photocured films in an oven at 75 °C for different times.

2.3. Characterization techniques

The kinetics of the photopolymerization process was investigated by using FT-IR spectrometry (ATI Mattson

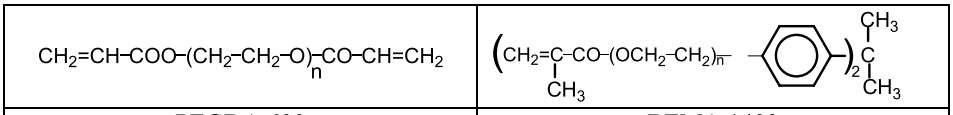

PEGDA 600	BEMA 1400

Fig. 2. Structure of PEGDA 600 and BEMA 1400.

Genesis II apparatus, USA), following the decrease of the band attributable to the acrylate and methacrylate groups at 1630 cm^{-1}. This band was normalized to the C=O signal located at 1700 cm^{-1}. The mixtures were coated onto a KBr disk and the curing reaction was monitored at different irradiation times.

The condensation reaction was followed by measuring the weight loss due to the alcohol evaporation (relative error = ±1%).

The gel content of the cured products was determined by measuring the weight loss of the samples contained in a metal net after 24 h extraction at room temperature with $CHCl_3$ (relative error = ±1%).

DSC measurements were performed using a Mettler DSC 30 (Switzerland) apparatus, equipped with a low temperature probe (heating rate: 20 °C/min). The mixtures were directly put into the Al crucibles and subjected to photochemical and condensation processes. T_g values were recorded during the 2nd heating scan. Some traces of water and alcohols were lost during the 1st scan. T_g values were calculated as the midpoint of the T_g step between onset and endpoint (error = ±1 °C).

Dynamic-mechanical analyses (DMTA) were performed on a MK III Rheometrics Scientific Instr. at 1 Hz frequency in the tensile configuration. The size of the specimen was about 14×9×0.1 mm. The storage modulus, E', and the loss factor, tan δ, were measured from −50 °C up to the temperature at which the rubbery state was attained. The T_g value was assumed as the maximum of the loss factor curve.

TGA analyses were performed using a LECO TGA-601 Instr. in the range between 20 and 950 °C, with a heating rate of 3 °C/min, in air.

RX measurements were performed using a Siemens D5000 diffractometer with the Cu Kα radiation (λ = 0.15406 nm).

TEM analyses were performed using a Philips 2010 microscope on microtomized specimens without any specific staining.

3. Results and discussion

3.1. Kinetic measurements

In Fig. 3 the FT-IR spectra of PEGDA system (containing 20% w/w of MEMO), before and after UV curing (time of irradiation: 40 s) are reported. It is evident the decrease of the band at 1630 cm^{-1}, attributed to the acrylic and methacrylic functionalities. In Figs. 4 and 5, the kinetic curves related to the decrease of the 1630 cm^{-1} band of PEGDA and BEMA systems are reported; an almost complete conversion of the unsaturations is achieved.

The kinetic curve of PEGDA system is higher with respect to BEMA. In fact it reaches the asymptotic value after 10 s irradiation, while BEMAs maximum conversion is observed after about 20 s. This result is in agreement with the higher polymerization rate of acrylic systems with respect to methacrylic ones [12]. The kinetics of photopolymerization for both the systems is not affected by the presence of 30% w/w of TEOS in the UV-curable mixture (Figs. 4 and 5).

The condensation reaction was followed by measuring the weight loss due to the alcohol evaporation (Fig. 6). The maximum of the condensation curve was achieved after 4 h treatment in an oven at 75 °C; in all the two systems investigated, the weight loss was very close to the stoichiometric value (27% w/w); PEGDA evidenced a slightly lower loss value (22% w/w). This result can be attributed to the higher condensation rate of PEGDA systems, which start to condensate at room temperature during their preparation.

The structure of the final network obtained after the dual-curing process can be schematized as reported in Fig. 7.

Concerning the PEGDA system, on the basis of the reactivity ratios of the acrylic and methacrylic double bonds reported in the literature [20], we can assume an almost random distribution of the acrylic and methacrylic units in the copolymer chains.

Hybrid films containing different amounts of TEOS in the range 10–50% w/w (with respect to the PEGDA or BEMA mixture) were prepared. The curing kinetic curves of these mixtures were found similar to those reported in Figs. 4 and 5.

3.2. Properties of the cured films

In Fig. 8 a typical DSC thermogram of a cured BEMA film containing 50% w/w of TEOS is reported. The glass transition region is evident, together with the absence of any PEO cristallinity.

In Table 1 the T_g values related to PEGDA and BEMA systems are collected. All the materials are amorphous. It is evident that T_g increases by increasing the TEOS content. The T_g values obtained by DMTA analyses show a similar trend, notwithstanding their higher values, which can be attributed to a frequency effect [21]. The T_g increase can be

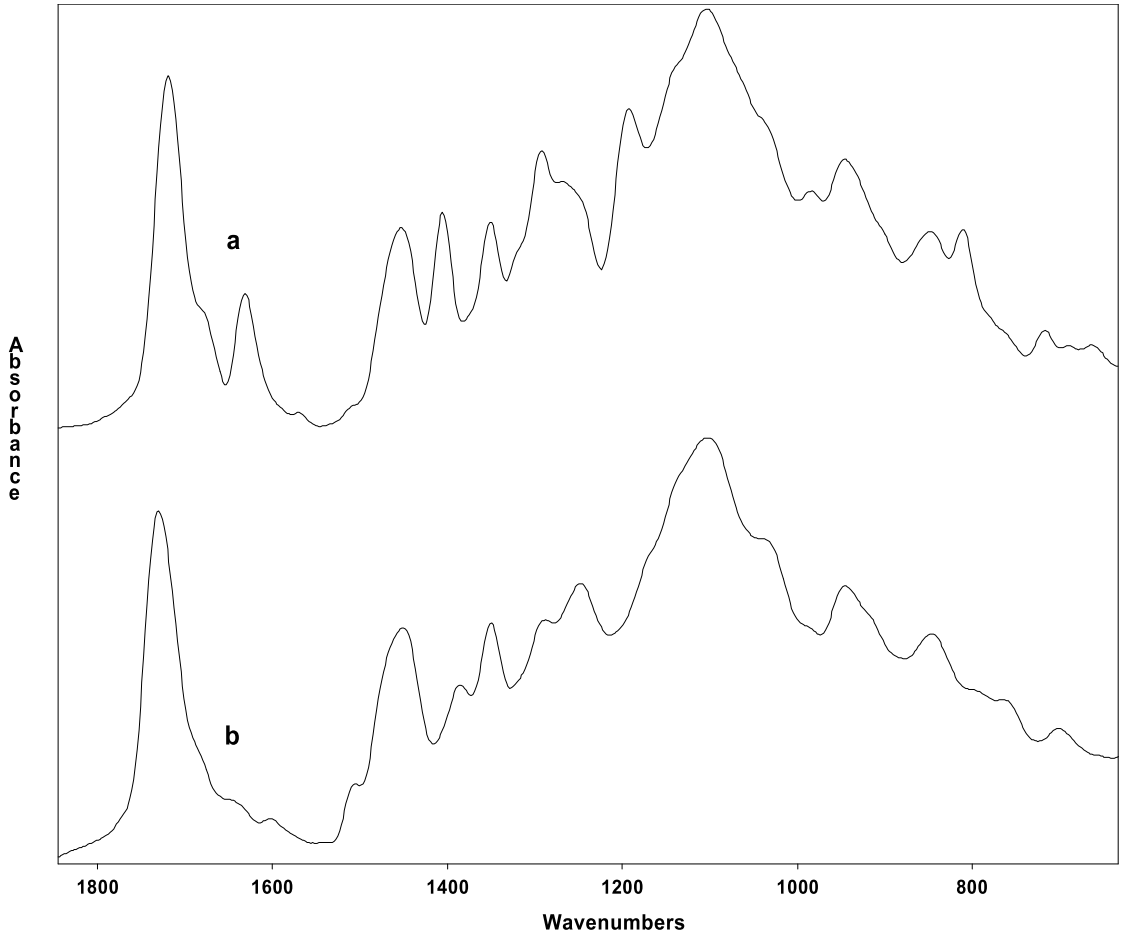

Fig. 3. FT-IR spectra of PEGDA system before (a) and after (b) UV curing (40 s irradiation).

attributed to the formation of the silica network, which induces constraints reducing the PEO segments mobility [21]. Moreover an increase of the storage modulus E', evaluated above the T_g value (40 °C) is observed: this can be due to the increase of the inorganic phase content, which acts as reinforcing agent. Two typical DMTA spectra of PEGDA and PEGDA +50% of TEOS are reported in Figs. 9 and 10, respectively.

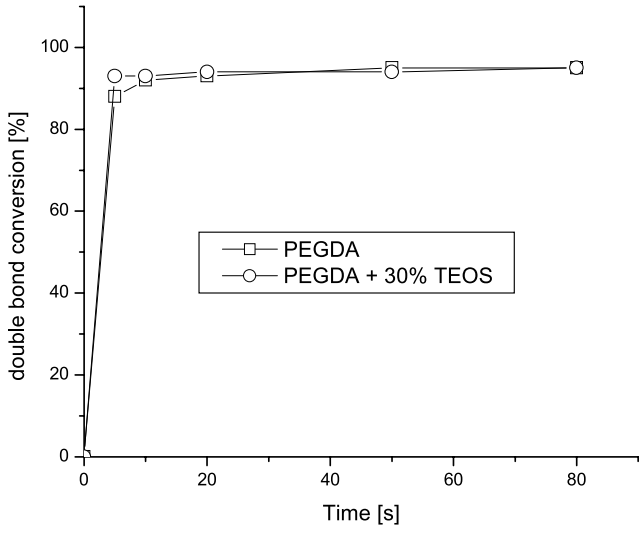

Fig. 4. FT-IR photopolymerization kinetic curves related to PEGDA and PEGDA+30% TEOS.

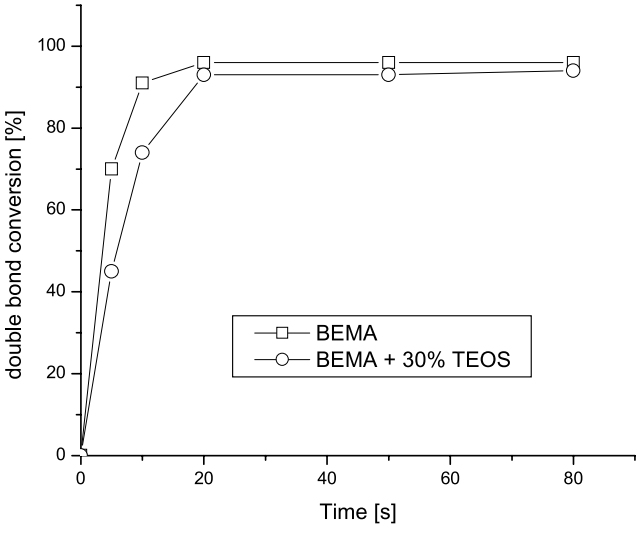

Fig. 5. FT-IR photopolymerization kinetic curves related to BEMA and BEMA+30% TEOS.

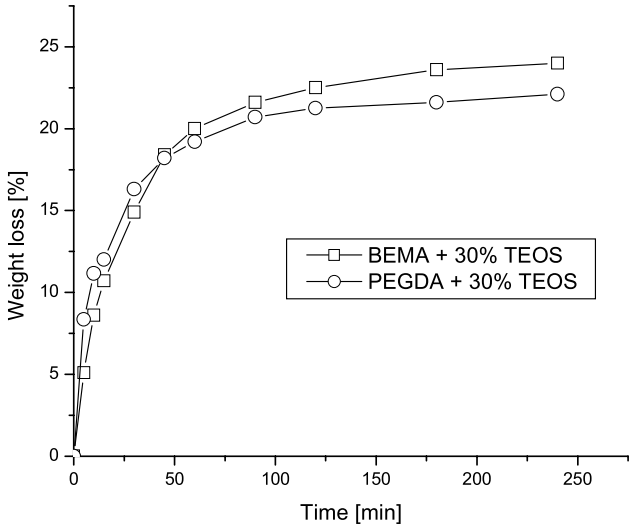

Fig. 6. Kinetic curves of the condensation reaction for PEGDA and BEMA systems containing 30% TEOS.

Table 1
T_g values of PEGDA and BEMA hybrid systems as a function of TEOS concentration

	T_g DSC (°C)	T_g DMTA (°C)	E' at 40 °C (MPa)
PEGDA	−36.0	−27.8	6
PEGDA + 10% TEOS	−28.0	−17.0	15
PEGDA + 30% TEOS	−23.0	−11.2	47
PEGDA + 50% TEOS	−15.0	−6.5	101
BEMA	−32.0	−23.2	14
BEMA + 10% TEOS	−24.5	−15.0	27
BEMA + 30% TEOS	−18.0	−5.6	76
BEMA + 50% TEOS	−8.0	+14.0	120

Further DMTA investigation will be published in a forthcoming work [22].

Moreover, BEMA-based systems show slightly higher T_g values with respect to PEGDA ones. This fact can be attributed to the presence of methacrylic double bonds in the polymeric chains; they give rise to higher T_g values with respect to acrylic double bonds [21]. Moreover, BEMA contains a rigid Bisphenol A structure in the middle of its molecule, which can induce an increase of the T_g value. On the other hand, we have to consider that BEMA 1400 has a higher MW with respect to PEGDA 600; thus a lower final crosslinking density of the network is achieved. As a consequence of these factors, a similar thermal behavior is observed.

In Table 2 the gel content of PEGDA- and BEMA-based systems having different amount of TEOS are collected before and after the thermal treatment. The data indicate that the thermal treatment induces an increase of the gel content, giving rise to an almost insoluble network.

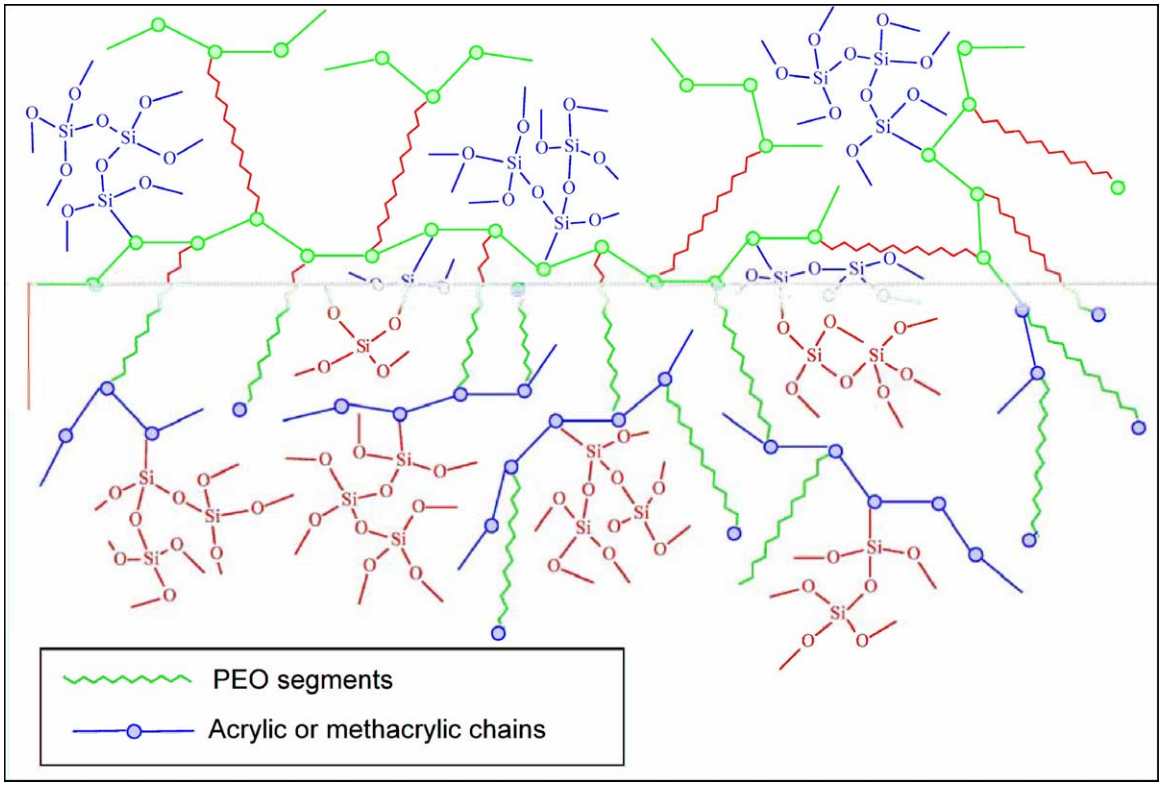

Fig. 7. Scheme of the final network obtained after photopolymerization and thermal condensation.

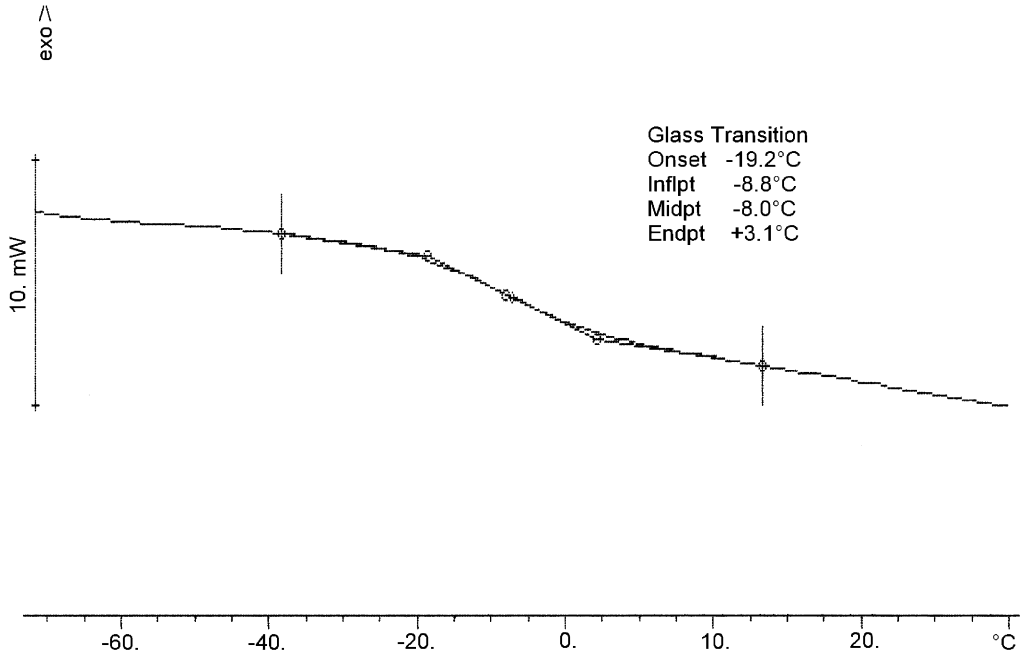

Fig. 8. DSC thermogram related to a BEMA + 50% TEOS hybrid.

The films are perfectly transparent. X-ray diffraction analyses indicate the absence of any crystallinity.

TEM micrographs evidence a phase separation at a nanometric level, as reported in Fig. 11. The presence of silica-rich phases is evident (their average dimension is about 20 nm). The mapping of Si through EDS technique showed the presence of higher Si content in the darker spots. Anyway, Si was also revealed in the lighter areas.

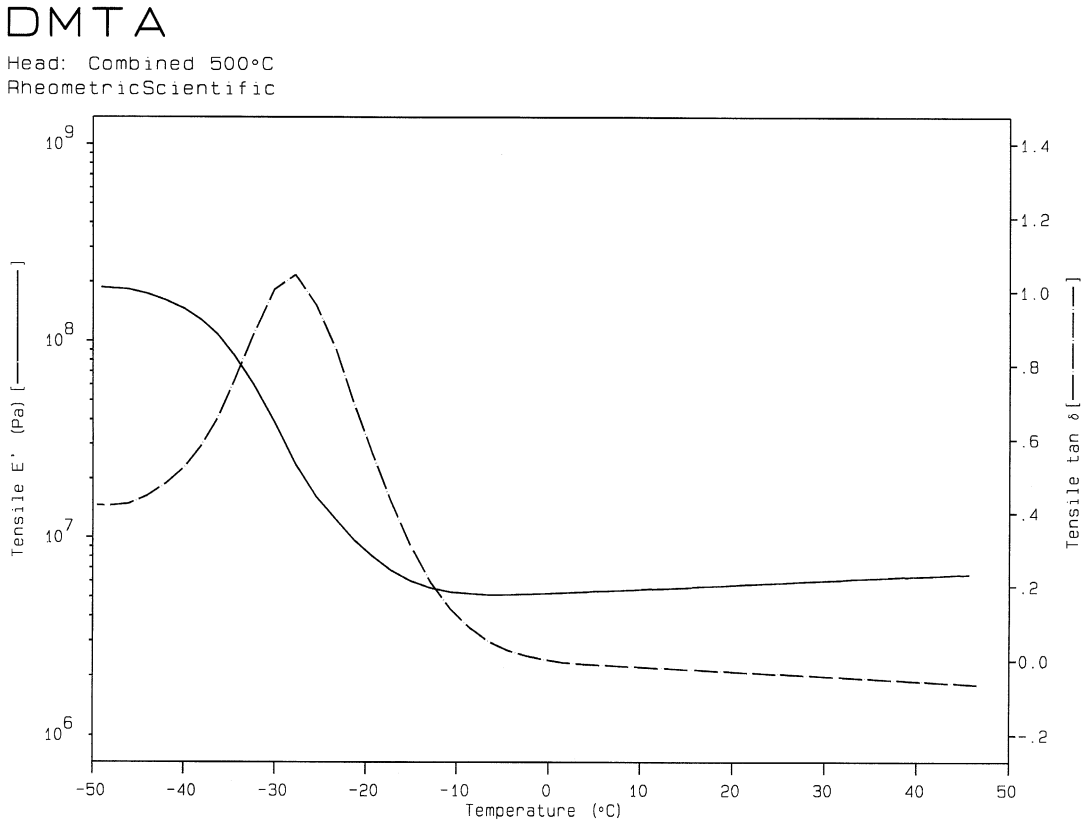

Fig. 9. DMTA spectrum related to a cured PEGDA system.

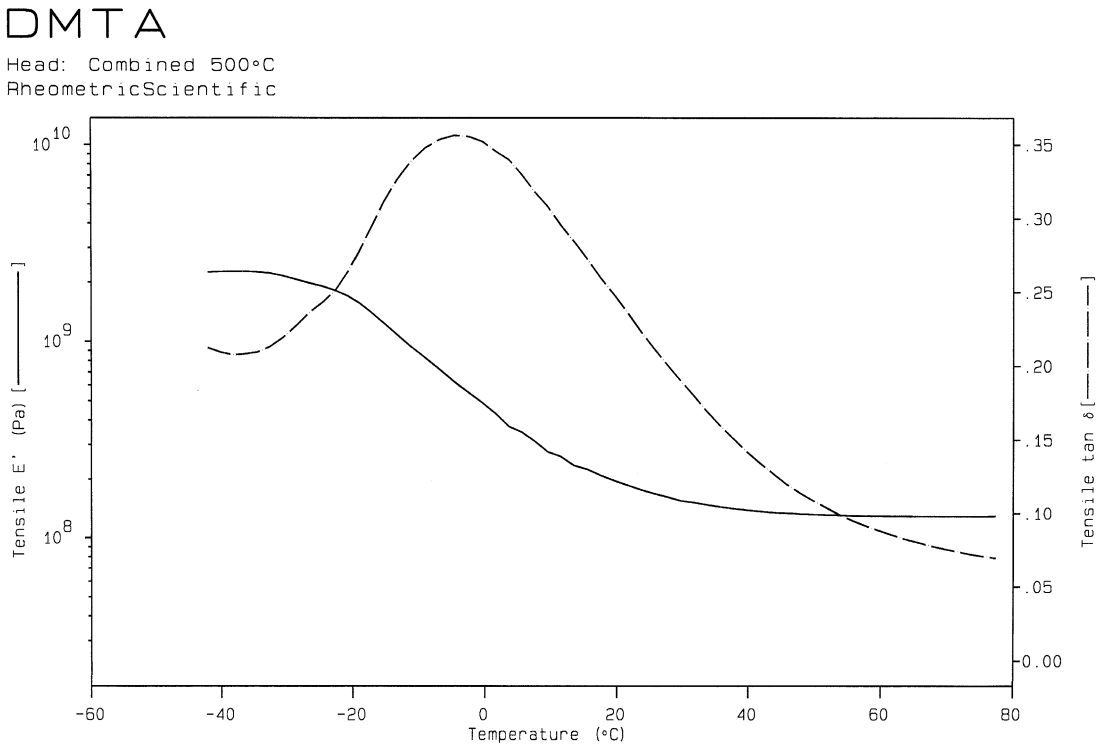

Fig. 10. DMTA spectrum related to a PEGDA+50% TEOS hybrid.

Moreover, some preliminary TGA experiments were performed in air and in N_2 in order to compare the thermal stability of the hybrid products with that of the systems not containing TEOS. The TGA curves reported in Fig. 12a for BEMA systems indicate a higher thermal stability of the hybrid systems with respect to those which do not contain TEOS. This behavior can be attributed to a slow down of the oxygen diffusion into the polymeric matrix, due to the presence of silica nanophases. By repeating the TGA analyses in N_2 (Fig. 12b) the two curves are superimposed until 500 °C, indicating the same thermal behavior.

4. Conclusions

Hybrid systems containing PEO segments linked to an acrylate–methacrylate network were prepared through a dual-curing process, which involves photopolymerization and condensation of alkoxysilane groups.

The evaluation of the acrylic and methacrylic groups and of the alkoxysilane groups (through the alcohol evaporation) indicated that an almost complete conversion of the reactive functional groups was achieved.

The T_g values of the hybrid films increased by increasing

Table 2
Gel content of the UV-cured materials before and after the thermal treatment (75 °C, 4 h)

Materials	Gel content (%)	
	Before	After
PEGDA	69	92
PEGDA+10% TEOS	81	94
PEGDA+30% TEOS	70	92
PEGDA+50% TEOS	67	96
BEMA	82	100
BEMA+10% TEOS	84	99
BEMA+30% TEOS	81	100
BEMA+50% TEOS	69	100

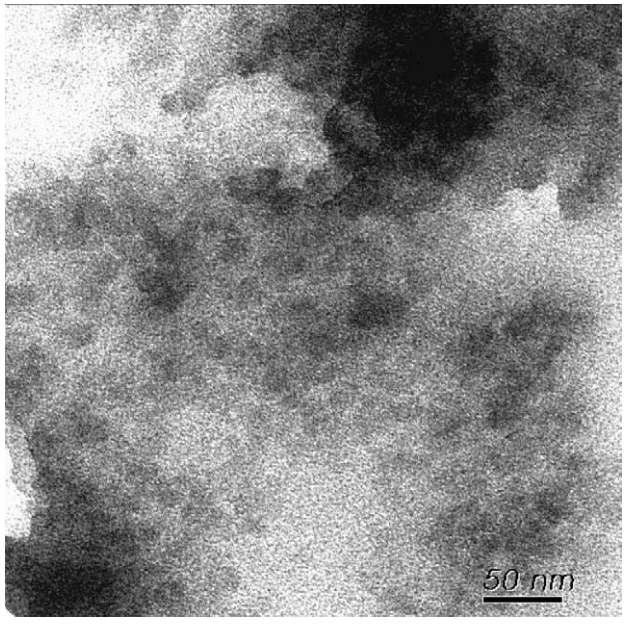

Fig. 11. TEM micrograph of a BEMA+30% TEOS hybrid.

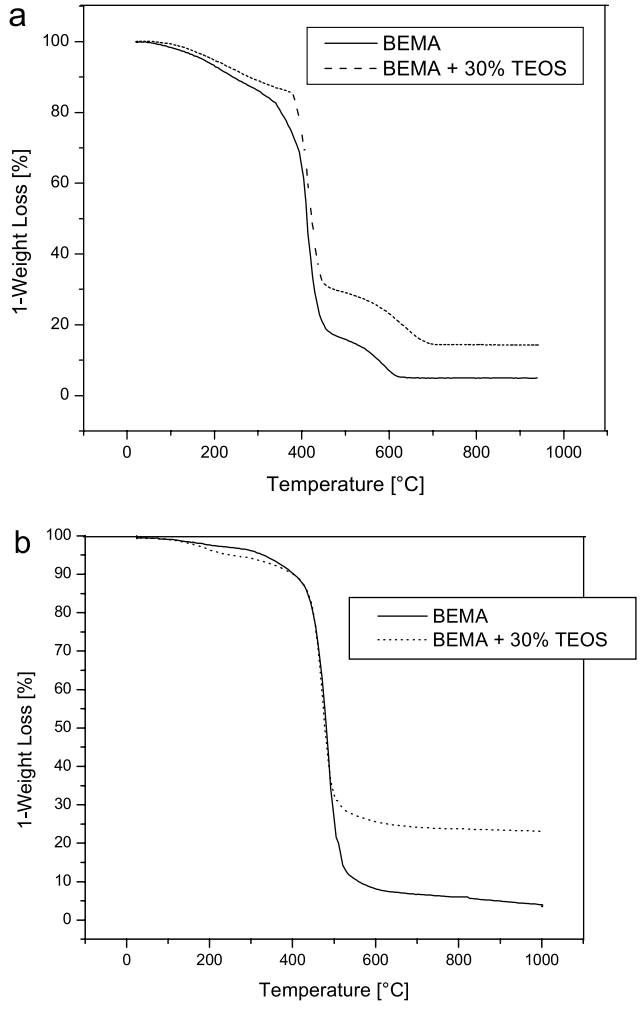

Fig. 12. TGA curves in air (a) and in N_2 (b) of cured BEMA and BEMA + 30% TEOS hybrid.

the amount of TEOS in the hybrid. This behavior can be explained considering the increase of constraints of PEO segments in the network due to the siloxane condensation reactions.

By comparing the thermal behavior of PEGDA and BEMA, higher T_g values were achieved by BEMA systems. This fact can be attributed to the presence in BEMA both of methacrylic double bonds and of the rigid structure of Bisphenol A.

The obtained films were perfectly transparent and amorphous; TEM analysis indicated the formation of silica phases at a nanometric level.

TGA curves revealed a higher thermal stability of the hybrid structures.

Acknowledgements

The financial support of INSTM Consortium (Florence, Italy), PRISMA 2003 project, is gratefully acknowledged.

References

[1] Yano S, Iwata K, Kurita K. Mater Sci Eng 1998;C:75–90.
[2] Wen J, Wilkes GL. Chem Mater 1996;8:1667–71.
[3] Mascia L. Trends Polym Sci 1995;3:61–6.
[4] Hajji P, David L, Gerard JF, Pascault JP, Vigier G. J Polym Sci: Part B: Polym Phys 1999;37:3172–9.
[5] Chang TC, Wang JT, Hong JS, Chiu YS. J Polym Sci: Part A: Polym Chem 2000;38:1772–7.
[6] Wei Y, Jin D, Xu J, Baran G, Qiu KY. Polym Adv Technol 2001;12: 361–8.
[7] Wu KH, Chang TC, Wang YT, Chiu YS. J Polym Sci Polym Chem 1999;37:2275–84.
[8] Zhu Z, Yang Y, Yin J, Qi Z. J Appl Polym Sci 1999;73:2977–84.
[9] Tian D, Dubois Ph, Jerome R. J Polym Sci Polym Chem 1997;9: 2295–309.
[10] Tian D, Dubois Ph, Jerome R. Polymer 1996;37:3983–7.
[11] Tian D, Blancher S, Dubois Ph, Jerome R. Polymer 1998;39:855–64.
[12] Tian D, Blancher S, Jerome R. Polymer 1999;40:951–7.
[13] Messori M, Toselli M, Pilati F, Fabbri E, Fabbri P, Busoli S, et al. Polymer 2003;44:4463–70.
[14] Cho J, Ju H, Hong J. J Polym Sci: Part A: Polym Chem 2005;43: 658–70.
[15] Glasel HJ, Bauer F, Ernst H, Findeisen M, Hartmann E, Langguth H, et al. Macromol Chem Phys 2000;201:2765–70.
[16] Zou K, Soucek MD. Macromol Chem Phys 2004;205:2032–9.
[17] Mark JE, Lee CYC, Bianconi PA. ACS Symp Ser 1995;585.
[18] Gigant K, Passet U, Schottner G, Baia L, Kiefer W, Popp J. J Sol–Gel Sci Techol 2003;26:369–73.
[19] Priola A, Gozzelino G, Ferrero F, Malucelli G. Polymer 1993;34(17): 3653–8.
[20] Brandrup J, Immergut EH, Grulke EA. Polymer handbook. New York: Wiley; 1999.
[21] Nielsen LE. Mechanical properties of polymers and composites. New York: Marcel Dekker; 1994.
[22] Ceccosulli G, Scandola M. In preparation.